eXPRESS Polymer Letters Vol.10, No.7 (2016) 587–597
Available online at www.expresspolymlett.com
DOI: 10.3144/expresspolymlett.2016.54

Improving the interfacial and mechanical properties of short glass fiber/epoxy composites by coating the glass fibers with cellulose nanocrystals

A. Asadi[1], *M. Miller*[1], *R. J. Moon*[2,3], *K. Kalaitzidou*[1,3*]

[1]G.W. Woodruff School of Mechanical Engineering – Georgia Institute of Technology, GA 30332 Atlanta, United States
[2]The Forest Products Laboratory, U.S. Forest Service, Madison, 53726 Wisconsin, United States
[3]School of Materials Science and Engineering – Georgia Institute of Technology, GA 30332 Atlanta, United States

Received 11 December 2015; accepted in revised form 11 February 2016

Abstract. In this study, the interfacial and mechanical properties of cellulose nanocrystals (CNC) coated glass fiber/epoxy composites were investigated as a function of the CNC content on the surface of glass fibers (GF). Chopped GF rovings were coated with CNC by immersing the GF in CNC (0–5 wt%) aqueous suspensions. Single fiber fragmentation (SFF) tests showed that the interfacial shear strength (IFSS) increased by ~69% in composites produced with CNC coated GF as compared to uncoated GF, suggesting an enhancement of stress transfer across the GF/matrix interface. The role of CNC coatings on the tensile, flexural, and thermo-mechanical properties of the CNC-coated GF/epoxy composites was investigated. Incorporation of 0.17 wt% CNC in the composite resulted in increases of ~10% in both elastic modulus and tensile strength, and 40 and 43 % in flexural modulus and strength respectively. In conclusion CNC coatings on GF alter the GF/matrix interface resulting in improvement of the mechanical performance of the corresponding composites.

Keywords: *polymer composites, nanomaterials, coatings, mechanical properties*

1. Introduction

Short glass fiber (GF) polymer matrix composites (PMC) with 30–50 wt% fiber loading have been widely used in automotive and marine industries as structural components due to their high specific strength and stiffness. Continued development in light-weighted PMC with higher mechanical performance has been fueled by the premise that 10% reduction in the vehicle weight can result in 6–8% increase in fuel efficiency [1]. One approach towards light weighting is the incorporation of nanoparticles either as a reinforcement phase within the matrix polymer, or at the fiber/matrix interface [2–5]. The high surface area per unit volume of nanoparticles enhances the interactions with the other constituents in the composite and subsequently enhances the mechanical properties compared to larger dimension particles of the same composition [6]. However, issues such as inhomogeneous dispersion and agglomerate formation should be addressed before using these materials in large scale production of composites.

Alternative nanoparticles that have potential for increasing GF-polymer matrix composites properties are cellulose nanomaterials (CNs). CNs are cellulose-based nanoparticles that are obtained from plants, algae, bacteria and marine animals [7–9]. CN particles are generally grouped based on the cellulose source and the extraction methods, leading to various CN types, including: cellulose nanocrystals (CNC), cellulose nanofibrils (CNF), algae cellulose (AC), bacterial cellulose (BC), etc. One common trait with all CN types is the parallel stacking of cellulose

*Corresponding author, e-mail: kyriaki.kalaitzidou@me.gatech.edu

chains along the particle length, and because of this feature the properties of the various CNs are similar to each other, at least within the scatter of experimental testing or atomistic model predictions [9]. With this in mind, as a whole CNs have a unique combination of characteristics [9] that make them attractive for certain composite applications, i.e. low density (1.6 g/cm^3), high surface area and aspect ratio (10–100), tensile strength of 3–7.5 GPa, and elastic modulus of 110–220 GPa, surfaces with accessible hydroxyl side groups (e.g. –OH) that can be readily chemically modified, and low toxicity [10]. In addition, CNs extracted from trees and plants have the potential to be produced at industrial scale quantities, and reasonable price [11]. In the current study, the CN type used was CNC, which are whisker-shaped particles (typically, 3–5 nm in width and 5–500 nm in length), extracted by acid hydrolysis of plants [12], and are considered to have properties within the ranges listed above.

There has been considerable interest in CNs as reinforcement in various polymer systems due to their high specific modulus and strength characteristics, and provided that the CNs are well dispersed within the polymer matrix, increases in mechanical performance of the CN-polymer system and subsequently the corresponding composites can be expected. For most epoxy systems, obtaining well dispersed CNs in epoxies has been exceedingly challenging, especially for high CN volume fraction [13–20]. To address this issues, waterborne epoxies [14, 15, 18], solvent exchange methods [20, 21], CN preforms impregnation [22] and chemical modification of CN surfaces have been used [23], however, the time and cost involved in these processes limit their capability in industrial scale production of GF/epoxy composites.

An alternative approach has been to add CNs to GF/epoxy composites by coating the GF prior to mixing into epoxy, where the CN coating modifies the GF/epoxy interface and subsequently improves the properties. A good review on tailoring interphase through coating the fibers in polymer composites can be found in [24]. Chen *et al*. [25] deposited bacterial cellulose (BC) on the surface of GF during the process of fermentation. The BC coated GF were subsequently compounded into epoxy, where the increase in the interfacial shear strength (IFSS) of BC coated GF/epoxy interface was attributed to the increase in interfacial surface roughness and area, and chemical bonding between the BC coating and the epoxy matrix. However, for large volume uses, growth of the BC film on GF is impractical. Additional work is needed to i) find coating processes that are quick, reliable, and inexpensive and ii) link changes in IFSS to differences in macroscopic mechanical properties of the GF/epoxy composites as a result of the addition of the CN coatings. To the best of the authors' knowledge, no studies exist on simple coating technique of GF with CN and the influence of the CN coating on both the interfacial and mechanical properties.

In this study, the effect of CNC coatings on GF on the GF/epoxy matrix interfacial properties and the subsequent influence on the mechanical properties of short GF/epoxy composites are investigated. GF were coated by immersing them in an aqueous CNC suspension (0–5 wt%), a scalable technique. Interfacial adhesion was characterized by the IFSS using single fiber fragmentation tests (SFF). Changes in the IFSS and stiffness across the GF/matrix interphase as a result of CNC coating on the GF were two potential mechanisms considered for the enhancement in tensile and flexural properties of CNC coated-GF/epoxy composites. The optimum CNC concentration on the GF that resulted in the best mechanical performance was determined.

2. Experimental details

2.1. Materials

Owens Corning (Oak Brook, IL, US) ME1510 multi-end roving GF (TEX 48000, single filament diameter of 10±1 μm) were used as received. The GF rovings were chopped to an average length of 25±0.5 mm. A bicomponent epoxy resin consisting of 635 thin epoxy and 556 slow amine hardener supplied by US Composites (West Palm Beach, FL) was used. CNC in the form of 11.9 wt% never-dried suspension in water [26] were supplied by the USDA Forest Service-Forest Products Laboratory (FPL), Madison, WI, USA. The average length and width of the CNC were 138±22 nm and 6.4±0.6, respectively [18].

2.2. Coating of GF with CNC and fabrication of CNC-coated GF/epoxy composites

CNC coated GF were produced by immersing ~154 g of chopped GF rovings in ~1000 mL of aqueous CNC suspension without agitation for 2 min, after which the GF were taken out and spread on covered trays with ample ventilation to dry 24 h at room temperature. This simple, low cost coating method is conceptually scalable for larger volume applications. The

CNC used were not functionalized or surface treated. For uncoated GF, a similar procedure was followed using distilled water with no CNC to maintain the consistency in fabrication. The CNC suspension was diluted, in order to adjust the CNC coating, using distilled water and then sonicated to achieve a uniform CNC dispersion in water. Sonication was carried out using Misonix S-4000 ultrasonic processor equipped with a 12.5 mm probe diameter at 30% amplitude and 20 W power for 8 min. Aqueous CNC suspensions of 0, 0.5, 1, 1.5, 2, 3 and 5 wt%, were prepared using the above procedure and used to coat the chopped GF rovings. The corresponding naming scheme used to describe the coated fibers is GF, 0.5S-GF, 1S-GF, 1.5S-GF, 2S-GF, 3S-GF, and 5S-GF, respectively. The 'S' in this case represents the concentration of CNC suspension.

For SFF test specimen preparation, individual GF filaments were carefully pulled off from the coated and uncoated GF rovings. Subsequently, a single 120 mm long GF filament was placed in the middle of a dog-bone shaped mold and covered with epoxy resin that was cured at 80 °C for 1 h, followed by post-curing at 100 °C for 4 h. Prior to pour the epoxy in the mold, the single GF filaments were manually pre-strained and the ends of the GF were taped down to ensure that the GF remain in tension during the epoxy curing. The resin was prepared by mixing the epoxy with hardener at 2:1 wt% using a VWR magnetic stirring plate at a 60 rpm, at room temperature for 10 min, and was degassed in a vacuum chamber for 5 min prior to pouring into the mold. SFF test specimens were prepared using the following GF: GF, 0.5S-GF, 1S-GF, 1.5S-GF, 2S-GF, 3S-GF, and 5S-GF. The SFF test dog-bone specimens were made according to the test protocol for SFF test [27], having a gauge length of 25 mm long, 3 mm wide and a depth of 2 mm, with an overall length and width of 80 and 10 mm, respectively.

GF/epoxy composites were produced with a 30 wt% GF content. Chopped GF rovings with or without CNC coatings were added and mixed with the resin using a spatula in a tote and degassed in a vacuum chamber, for 5 min. Then, the mixture was spread in a rectangular mold and cured as described above. Based on the SFF results (see Section 3.2), only 1S-GF, 1.5S-GF and 2S-GF were used to make CNC-GF/epoxy composites. The test coupons were cut from the plate using a waterjet (MAXIEM 1515).

2.3. Characterization techniques

2.3.1. Single-fiber fragmentation tests (SFF)

SFF tests, as described by Hunston *et al*. [27], were used to quantify the effect of CNC coatings on the IFSS. In brief, tensile tests, with applied load along the fiber axis direction, were carried out at a displacement rate of 1 mm/min using an Instron 33R 4466 equipped with a 500 N load cell. The tests continued until the load passed its peak and dropped at 90–95% of maximum load to ensure that no further fiber fragmentation could occur. Since the GF were pre-strained, it was expected that when the epoxy reached at its strain to failure, saturation in the GF fragmentation had occurred. It is noted that if the test continued further than this point, the samples would break into two pieces and the fragmentation lengths could not be recorded. The IFSS was determined by Kelly and Tyson model [28] given in Equation (1):

$$\tau_{\mathrm{i}} = \frac{d_{\mathrm{f}}\sigma_{\mathrm{f}}(l_{\mathrm{c}})}{2l_{\mathrm{c}}} = \frac{3d_{\mathrm{f}}\sigma_{\mathrm{f}}(l_{\mathrm{c}})}{8\bar{l}} \tag{1}$$

where τ_{i} is the IFSS, d_{f} is the fiber diameter, l_{c} is the fiber critical fragmentation length, $\bar{l}$ is the average length of fiber fragmentation segments ($l_{\mathrm{c}} = 4\bar{l}/3$) and σ_{f} is the fiber strength at the critical length. The fiber diameter and fiber fragmentation lengths were measured using polarized microscopy. The GF fiber strength was estimated by tensile testing (ASTM D3822), where a single GF fiber was attached to a paper tab and tested at a displacement rate of 1 mm/min using the Instron. An average GF strength of 2900±350 MPa was measured for a gauge length of 25.4 mm and as expected, the CNC coating process did not affect the single GF ultimate strength. Both the strength value and the IFSS values reported are an average of at least 10 measurements. Weibull distribution was applied for the GF strength data [29] to obtain the Weibull modulus and fiber strength as 4.57 and 2900 MPa respectively. These values were used to extrapolate the GF strength at the critical length required in Equation (1).

2.3.2. Microscopy

A Leica DM2500 polarized light optical microscope was used to characterize CNC coatings on chopped GF rovings, and to measure the fiber fragmentation lengths in SFF tests. A Hitachi SU 8230 field emission scanning electron microscope (FE-SEM) at an acceleration of 5 kV were used to view the CNC coat-

ings on individual GF, and the fracture surfaces of the composites. A plasma sputter (Ted Pella Inc.) was used to apply gold coating on the surface of the samples prior to SEM imaging to minimize charging.

2.3.3. Specific density, thermal stability and CNC content

Water displacement method was used to measure the specific density of the composites according to ASTM D-792. Thermogravimetry analysis (TGA), using TGA SDT Q600 (TA Instruments), was used to assess the thermal stability of CNC and determine the CNC content on the GF. The samples were heated from 50 to 500 °C at 10 °C/min in inert atmosphere. Each data point is an average of at least 3 measurements.

2.3.4. Mechanical and dynamic mechanical testing

The tensile properties of the composites were determined according to ASTM D638 using an Instron 33R 4466 equipped with 10 kN load cell. An extensometer, Instron 2630-35, with a gauge length of 50.8 mm was used. The modulus was calculated between the axial strain values of 0.05 and 0.2%. Each tensile data point is an average of at least five samples. The flexural properties were measured using three-point bending tests with an Instron 33R 4466 equipped with 10 kN load cell according to ASTM D790-02 with a support span of 50 mm and a sample thickness of 5 mm at a displacement rate of 0.85 mm/min. Each flexural data point is an average of at least seven tests. Dynamic mechanical thermal analyses (DMA Q800, TA Instruments) in three-point bending mode was used to measure the storage and loss moduli and the glass transition temperature (T_g) in the 25–160 °C range at a heating rate of 5 °C /min and 1 Hz. A preload of 0.01 N and a maximum strain of 0.05% were applied on the specimens. Each data point is an average of at least five tests.

3. Results and discussion

In order to test the hypothesis that addition of CNC on the GF/epoxy interphase can improve the mechanical properties of the composites, composites with uncoated and CNC coated GF were compared in terms of mechanical properties. First, it was determined whether or not the CNC alter the GF/epoxy interphase (a region around the GF in which the mechanical properties differ from the bulk mechanical properties of the composite) and the optimum CNC concentration needed to increase the properties of the composites with no weight penalty.

3.1. CNC coatings on GF

GF rovings were coated with CNC according to the process described in Section 2.2. As shown in Figure 1a, 1b, a thin layer of CNC is deposited on the GF surface as a result of physical absorption (e.g. hydrogen bonding of the accessible –OH side groups on the CNC surface as described in Chen *et al*. [25]). Of interest is how the CNC coated the chopped GF rovings, as well as individual GF within the rovings. To observe the surface of individual GF, the GF were pulled out from the chopped GF rovings after the coating process. As shown in Figure 1c–e, the uncoated GF has a smooth surface, while the surface of CNC coated GF is rougher, indicating that CNC have been deposited on the GF surface. Additionally, the coated GF surface roughness appears to increase with the CNC coating deposition concentration, suggesting that more CNC are deposited on the GF surface. Some of the roughness features in the CNC coating on individual GF is likely associated with the CNC coating process using the GF rovings as opposed to individual GF, in which GF-GF meniscus formation within GF rovings during drying would cause deposition variations. In addition, deformation of the CNC coating would occur when separating GF from other GF within the GF roving.

The implications of these observations are that although GF rovings are used in the coating process, the CNC suspension can penetrate the GF rovings and coat individual GF. The differences in the GF surface roughness of individual GF may subsequently alter the stress transfer efficiency at the GF/epoxy interphase in SFF testing that uses individual GF, as seen in Section 3.2, but it is unclear to what extent, roughness will influence the results of the composites testing where much larger-sized chopped GF rovings are used.

3.2. Interfacial properties

Figure 2a shows an optical image of a post-tested SFF 0.5S-GF test coupon with three fracture events along the GF, where the distance between each fracture represents an individual fiber fragment length. The average fiber critical length (= $4\bar{l}/3$, where $\bar{l}$ is the average of several individual fiber fragment lengths), and the calculated IFSS, as a function of

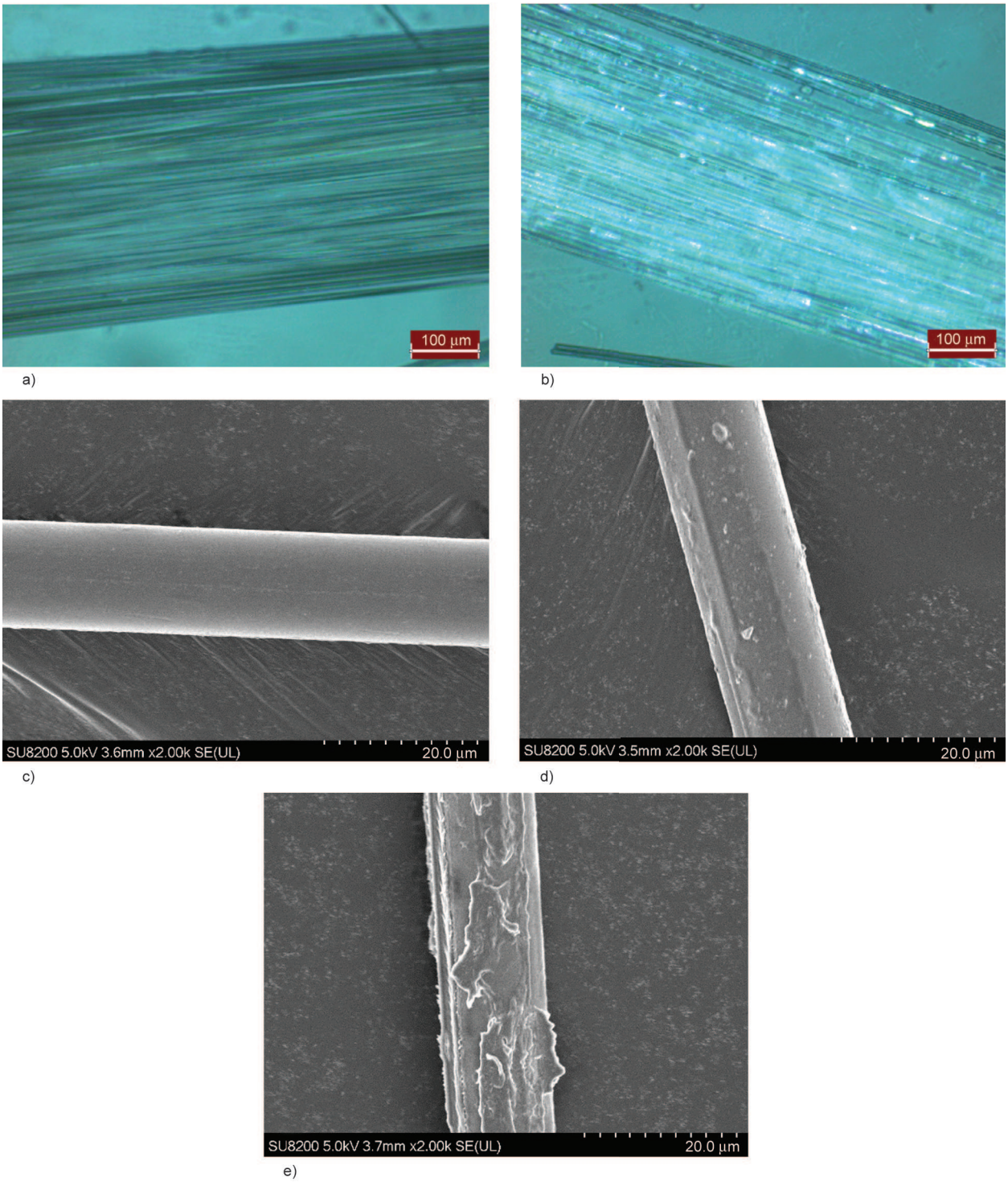

Figure 1. Polarized micrographs (polarized light of 95°) of chopped GF rovings, (a) uncoated, and (b) coated 1.5S-GF; SEM images of single GF coated with CNC (c) 0 wt%, (d) 1 wt % and (e) 5 wt% suspensions

CNC coating concentration on the GF surface are shown in Figure 2b. Changes in both the IFSS and fiber critical length when the GF are coated indicate that the load transfer across the GF/CNC/epoxy interphase has been modified. Possible mechanism are mechanical interlocking between the GF and epoxy due to the increased GF surface roughness and corresponding increased surface area, as well as different chemical affinity as a result of the GF having a CNC coating. There appears to be an optimum condition i.e. 1S-GF for which the IFSS reaches a maximum, that corresponds to ~69% increase compared to that of the uncoated GF/epoxy specimen. As the concentration of CNC suspension increases, i.e. for 1.5S-GF, 2S-GF, 3S-GF, and 5S-GF SFF cases, there is a reduction in IFSS. The lower IFSS suggest that

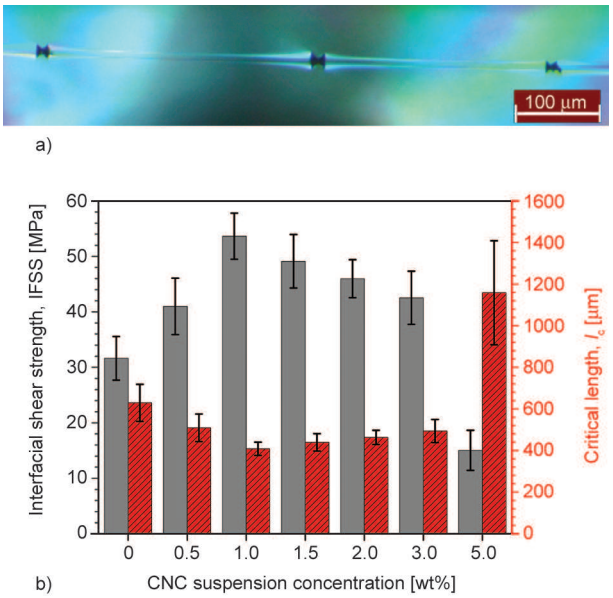

Figure 2. SFF results: (a) Polarized light micrograph of a single GF coated with 0.5CNC-GF (polarized light 80°) embedded in epoxy showing representative critical fragmentation length, (b) Interfacial shear strength (solid gray bars) and critical fragmentation length (striped red bars) for composites as a function of CNC suspension concentration. Error bars are 1 standard deviation.

the CNC coatings have reduced the stress transfer efficiency at the GF/CNC/epoxy interphase. A few mechanisms are plausible, which can be based on the quality of the CNC coating and associated interfacial defects. As shown in Figure 1e, 5S-GF tend to have rougher surfaces and other defects within the CNC coating, e.g. formation of CNC multilayer that can potentially result in slippage of CNC with respect to each other and reduction of the stress transfer efficiency.

There were various fracture modes observed for the specimens with different CNC coating contents, suggesting that there is a change in the interfacial properties at the GF-epoxy interface caused by the CNC coatings. According to Mullin and Mazzio [30], fracture modes in single fiber fragmentation tests can be categorized to three modes based on the fiber/matrix level of adhesion; *mode i:* following the fiber break, a disk shaped matrix crack occurs as a result of normal stresses, shown in Figure 3a, suggesting a strong interface; *mode ii:* following the fiber break, a double cone-shaped matrix crack with 45° angle occurs as a result of shear stresses, shown in Figure 3b, referring to a type of interface in which the matrix shear strength is lower than its tensile strength; and *mode iii:* fiber break is instantly followed by a limited interfacial debonding due to shear stress, shown in Figure 3c, implying a weak interface type. The debonded interface cannot transfer any load from matrix to the fiber and the length of debonding can be used as an indicator of fiber stress and interfacial energy [31]. For epoxies, concurrent disk-shaped and cone-shaped matrix cracks formed at the fiber ends are commonly seen. In the current study, combined fracture *modes i* and *ii* along with few cracks of mode iii were observed for the GF and 0.5S-GF samples, as shown in Figure 4a–c. The fracture mode for 1S-GF, 1.5S-GF, 2-S-GF, and 3S-GF SFF samples were combined modes i and ii, shown in Figure 4d, 4e, suggesting a stronger interfacial bonding compared to uncoated-GF/epoxy samples. The fracture modes for 5S-GF samples were *mode ii* and *mode iii;* however, it was observed that the debonded areas increased compared to that of uncoated GF/epoxy samples implying a weaker interface and a lower IFSS value, as seen in Figure 2.

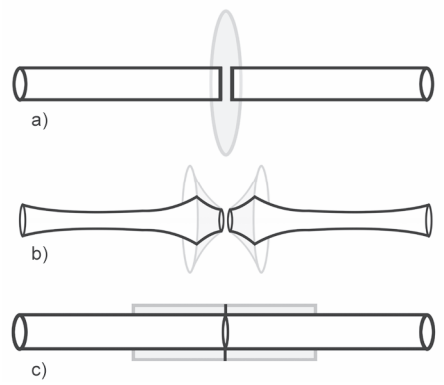

Figure 3. Three modes of fracture in matrix in single fiber fragmentation test; (a) *mode i:* disk-shaped fracture of matrix referring to strong interface, (b) *mode ii:* double-cone matrix fracture suggesting a matrix with a low shear strength, and (c) *mode iii:* debonding of fiber and matrix inferring a weak interface

3.3. Specific density, CNC content and thermal stability

GF/epoxy composites were made using the following chopped GF rovings: GF, 0.5S-GF, 1S-GF, 1.5S-GF and 2S-GF. The density for all these composites was found to be 1.3±0.03 g/cm^3, delineating that the CNC coatings did not significantly increase the composite weight and is consistent with the small CNC wt% deposited on the GF.

The CNC wt% within chopped GF rovings as well as within the composites was correlated with the CNC suspension concentration used in the coating

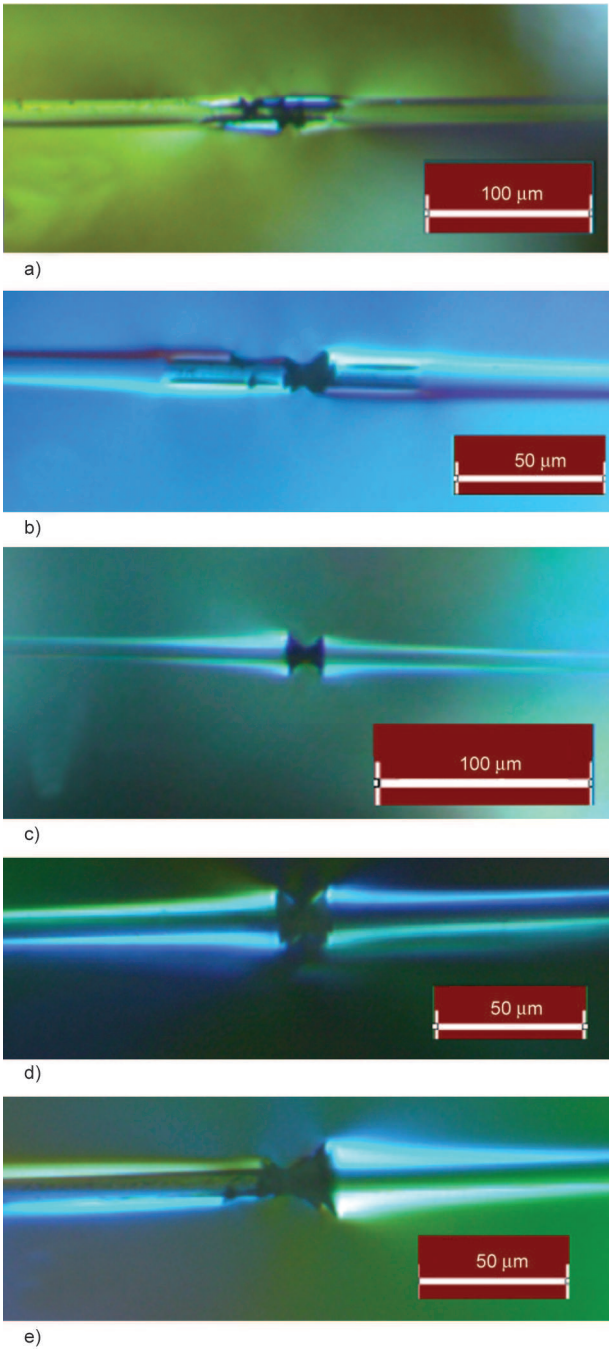

Figure 4. Optical polarized light micrographs of SFF specimens after tensile test showing fracture events at the GF: (a) GF/epoxy (polarized light of 75°), (b) 0.5S-GF (polarized light 120°), (c) 0.5S-GF (polarized light 80°), (d) 1S-GF (polarized light 90) and (e) 2S-GF (polarized light 75°)

process as shown in Figure 5. The uncoated GF used as the baseline for determining the CNC wt% on the coated GF. The CNC content on the GF surface increased from 0.44±0.07 to 3.58±0.02 wt% for 0.5 and 5 CNC wt% suspensions, respectively. It is noted that the CNC wt% on the GF surface is not increasing linearly with the CNC suspension concentration

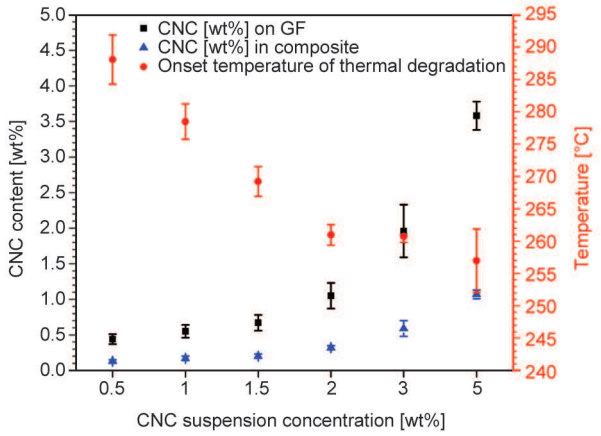

Figure 5. CNC suspension concentration on the GF and composites and onset temperature of thermal degradation for CNC-coated GF as a function of CNC concentration in the aqueous solution. Error bars are 1 standard deviation

used in coating process, e.g. the CNC content on the GF coated with 1 CNC wt% solution is not twice of that of the GF coated with 0.5 CNC wt%.

The thermal stability of the CNC-coated GF is also plotted in Figure 5. The onset temperature of thermal degradation of the neat CNC was 234.23±0.67 °C. All the coated-GF degraded above this temperature (lower bound). The onset temperature of thermal degradation decreased with the increase in the CNC content on the GF which was expected as it should reach the lower bound with the increase in the CNC content.

3.4. Fracture surface morphology

The fracture surface of the composites failed in the tensile testing was studied using a FE-SEM. As shown in Figure 6a, 6b, the main failure mechanism for uncoated GF epoxy composites was interfacial debonding as indicated by the clean pulled-out fibers devoid of the matrix, suggesting weak fiber-matrix adhesion. In contrast, the failure mechanisms for CNC-coated GF epoxy composites were concurrent matrix cracking, fiber breakage and interfacial debonding, shown in Figure 6c, 6d, implying an improvement in the interfacial bonding as a result of CNC coating. Also, matrix residues on the pulled-out fibers (Figure 6d) and a rough fracture surface for both 1S-30GF/epoxy and 2S-30GF/epoxy composites compared to the smooth fracture surface for the uncoated GF/epoxy composites suggest a better adhesion between fiber and matrix.

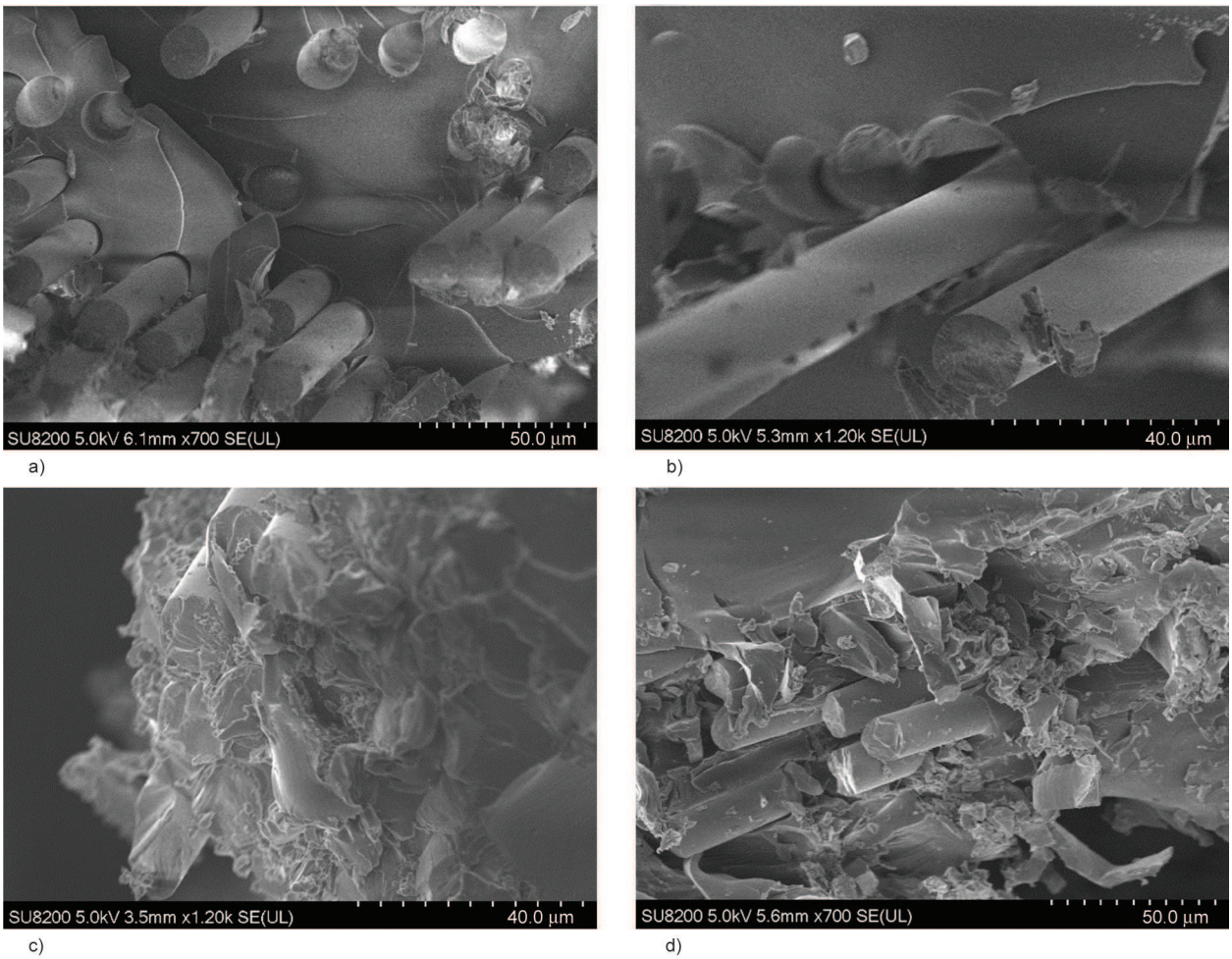

Figure 6. SEM images for fracture surface of different epoxy composites; (a) and (b) uncoated 30GF/epoxy, (c) 1S-30GF/epoxy, (d) 2S-30GF/epoxy

3.5. Tensile and flexural properties

The effect of the CNC content on the tensile and flexural properties of CNC coated GF/epoxy composites are plotted in Figure 7. The incorporation of CNC as a coating to GF enhances the elastic modulus by ~10% for 1S-30GF/epoxy and 1.5S-30GF/epoxy composites with respect to that of uncoated GF/epoxy. This may be a result of the increase in the stiffness of the GF/epoxy interphase due to presence of CNC as according to Hashin [32], for an imperfect interface (i.e. displacement discontinuity across the interface) an interfacial stiffness parameter can be defined where a higher value of this parameter suggests a faster rate of stress transfer across the fiber/matrix interface and thus a higher modulus for the composite [33]. Although this hypothesis could not be validated in this study, Gao and Mäder [34] showed how increases in the apparent modulus at the GF/epoxy interphase resulted in increase in the composite macroscopic modulus, which can be qualitatively linked to the current study where enhancement in the apparent modulus of the GF/epoxy interphase resulted in higher macroscopic modulus of the composites. In addition, the tensile strength increased for 1S-30GF/epoxy (~10%) and 1.5S-30GF/ epoxy composites with respect to that of 30GF/ epoxy composites. This increase reflects the higher IFSS (see Figure 2) inferring stronger interfacial interactions and better stress transfer across the fiber/CNC/epoxy interphase as also reported elsewhere [35]. The tensile strength of the 2S-30GF/epoxy composite was ~12% lower despite having higher IFSS compared to that of 30GF/epoxy. This may be due to various mechanisms including void formation within and around the GF rovings as a result of incomplete infiltration of the epoxy within the coated GF rovings and breaking of the CNC coating as it becomes more brittle with increase of its thickness. The strain at break had a trend similar to that of the strength, where the strain at break in 1S-30GF/epoxy and

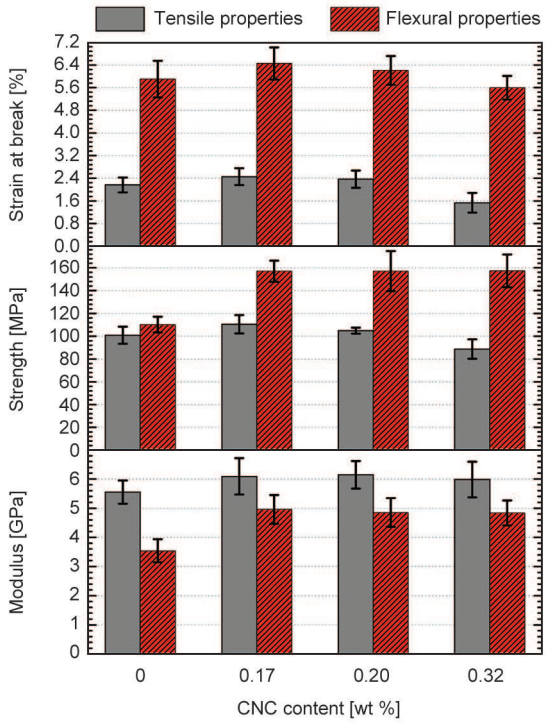

Figure 7. Effect of the CNC content (wt% in composite) in CNC-coated 30GF/epoxy composites on tensile and flexural properties. Error bars are 1 standard deviation

1.5S-30GF/epoxy composites increased by ~14 and ~10% while that of 2S-30GF/epoxy decreased compared to uncoated 30GF/epoxy composites.

For composites made with 1S-GF and 1.5S-GF, the flexural modulus and strength increased by ~40 and ~42%, respectively, with respect to those of uncoated 30GF/epoxy composites indicating better adhesion between the glass fiber and epoxy due to higher IFSS, and stress transfer at a faster rate as discussed above. The strain at break follows similar trend to that of axial strain, where it increased by ~10% for 1S-30GF/epoxy.

It is noted that the enhancement in flexural properties was larger than the enhancement in tensile properties at the same CNC content. The differences in elastic moduli and strengths may result from the difference in tensile and flexural moduli of the epoxy resin. In most epoxy systems, the tensile modulus is higher than the flexural modulus while the tensile strength is lower than the flexural strength (e.g. report by Kinsella *et al.* [36]). In addition, for the strength and the strain at break, a different mechanism may be at play since these properties are typically dominated by defects within the composite. For materials with defect mediated failure, strength and strain at break properties will be dependent on the number of defects, their size, where they are located with respect to the high stressed portions of the sample and volume subjected to the highest tensile stress. For the samples used in tensile and flexural testing, it is likely that the defect numbers and size distributions are similar in all samples tested; however, in the tensile coupons, all the material in the gauge portion experiences the maximum stress as compared to the to the flexural sample configuration in which only the outer surfaces of specimen are subjected to the maximum stress. With this in mind, for the tensile testing, there is higher probability that a larger number of defects is located in the high tensile stressed portions of the sample and because of this, a lower applied load would be needed to induce fracture. Moreover, the larger enhancement of the flexural properties compared to the enhancement of the tensile properties can be due to the fact that the glass fibers are randomly oriented in plane so that in tensile loading only a portion of their length along the direction of the applied load will bear loading. In case of the three-point bending, the load direction is out of plane and all the fibers (across the whole length) are available to take up load and therefore enhancement in the flexural properties would be higher.

3.6. Dynamic thermo-mechanical properties

The dynamic thermo-mechanical properties of the composites below and above T_g are presented in Table 1. At 25 °C, the incorporation of CNC as a coating to GF rovings was shown to enhance the storage modulus (E') for the 1S-30GF/epoxy and 1.5S-30GF/epoxy composites, but lower the storage modulus for 2S-30GF/epoxy composites, as compared to that of 30GF/epoxy composites. The increase in the storage modulus at 25 °C can be attributed to the stiffening of the GF/CNC/matrix interphase due to presence of CNC particles, as discussed in Section 3.5. Although the average value of the rubbery moduli (E_r: the storage modulus above T_g) measured at 90 °C for the composites containing CNC-coated GF were lower than that of the composite incorporating uncoated GF, due to the large standard deviation in measured properties, it was concluded that coating of the GF with CNC did not impact the rubbery modulus. Studies have shown that addition of CNC in the epoxy increased the rubbery modulus due to the formation of a network of mechanically percolated CNC [16, 18, 21]. However, it is expected that CNC on the surface of the GF do not form a percolated network

Table 1. Viscoelastic properties of CNC-GF/epoxy composites in three-point bending mode

Composite	E' at 25 °C [MPa]	E_r at 90 °C [MPa]	T_g [°C]	tan δ at T_g
30GF/epoxy	4932±586	250±21	50.3±0.7	0.61±0.06
1S-30GF/epoxy	5213±543	224±31	49.4±0.5	0.61±0.02
1.5S-30GF/epoxy	5614±695	228±22	50.2±0.8	0.65±0.07
2S-30GF/epoxy	4634±257	243±38	49.5±1.1	0.59±0.02

E': storage modulus
E_r: rubbery modulus
T_g: glass transition temperature measured in tan δ peak
tan δ: value of tan δ peak
Note: Error bars are 1 standard deviation.

within the polymer matrix. Hence, CNC cannot strongly impact the polymer chain segmental motion and consequently, the rubbery modulus. Presence of CNC has no effect on the tan δ and the glass transition temperature (T_g).

4. Conclusions

This study demonstrated that introducing a small amount of CNC in the form of a coating on GF can enhance the IFSS and mechanical properties of short GF/epoxy composites without increasing the weight. The proposed mechanism for altering the composite properties is the improvement of the interfacial adhesion and stress transfer ability and rate across the GF/epoxy interphase due to the CNC coating. Single fiber fragmentation tests showed that coating of GF up to 1.96 wt% (coated in 3 wt% aqueous CNC suspension) was able to increase IFSS; however, the highest increase in IFSS (by 69%) was achieved for CNC coating of 0.55 wt% (coated in CNC 1 wt% aqueous CNC suspension). The CNC-GF/epoxy composites produced using CNC coated chopped GF roving showed increases in tensile and flexural properties, which were attributed to the increase in IFSS associated with the application of the GF coatings. The greatest improvement in properties occurred when CNC coating on GF rovings equal to 0.17 wt% of composite was used. Specifically, the tensile elastic modulus and strength by ~10%, tensile strain at break by ~14%, the flexural modulus and strength by ~40% and flexural strain at break by ~10%. It is noted that the CNC coating did not significantly alter the rubbery modulus, T_g and tan δ. The results highlight that the use of CNC coatings on GF, is a possible approach for enhancing the mechanical properties of GF/epoxy composites with no weight penalty.

Acknowledgements

This work was supported by funding from P^3 Nano and the U.S. Endowment for Forestry and Communities. The authors would like to thank Prof. Jon Colton for providing mechanical testing equipment.

References

[1] U. S. Department of Energy: The quadrennial technology review. p.39 (2011).
[2] Dorigato A., Morandi S., Pegoretti A.: Effect of nanoclay addition on the fiber/matrix adhesion in epoxy/glass composites. Journal of Composite Materials, **46**, 1439–1451 (2012).
DOI: 10.1177/0021998311420311
[3] Pedrazzoli D., Pegoretti A., Kalaitzidou K.: Synergistic effect of exfoliated graphite nanoplatelets and short glass fiber on the mechanical and interfacial properties of epoxy composites. Composites Science and Technology, **98**, 15–21 (2014).
DOI: 10.1016/j.compscitech.2014.04.019
[4] Pedrazzoli D., Pegoretti A.: Silica nanoparticles as coupling agents for polypropylene/glass composites. Composites Science and Technology, **76**, 77–83 (2013).
DOI: 10.1016/j.compscitech.2012.12.016
[5] Gao S-L., Mäder E., Plonka R.: Nanocomposite coatings for healing surface defects of glass fibers and improving interfacial adhesion. Composites Science and Technology, **68**, 2892–2901 (2008).
DOI: 10.1016/j.compscitech.2007.10.009
[6] Luo J-J., Daniel I. M.: Characterization and modeling of mechanical behavior of polymer/clay nanocomposites. Composites Science and Technology, **63**, 1607–1616 (2003).
DOI: 10.1016/S0266-3538(03)00060-5
[7] Hubbe M. A., Rojas O. J., Lucia L. A., Sain M.: Cellulosic nanocomposites: A review. BioResources, **3**, 929–980 (2008).
[8] Habibi Y., Lucia L. A., Rojas O. J.: Cellulose nanocrystals: Chemistry, self-assembly, and applications. Chemical Reviews, **110**, 3479–3500 (2010).
DOI: 10.1021/cr900339w
[9] Moon R. J., Martini A., Nairn J., Simonsen J., Youngblood J.: Cellulose nanomaterials review: Structure, properties and nanocomposites. Chemical Society Reviews, **40**, 3941–3994 (2011).
DOI: 10.1039/C0CS00108B
[10] Roman M.: Toxicity of cellulose nanocrystals: A review. Industrial Biotechnology, **11**, 25–33 (2015).
DOI: 10.1089/ind.2014.0024
[11] Hansen, F., Brun, V., Keller, E., Wegner, T., Meador, M., Friedersdorf, L.: Cellulose nanomaterials-A Path towards commercialization. USDA Forest Service Workshop report, Washington (2014).
[12] Beck-Candanedo S., Roman M., Gray D. G.: Effect of reaction conditions on the properties and behavior of wood cellulose nanocrystal suspensions. Biomacromolecules, **6**, 1048–1054 (2005).
DOI: 10.1021/bm049300p

[13] Lee K-Y., Aitomäki Y., Berglund L. A., Oksman K., Bismarck A.: On the use of nanocellulose as reinforcement in polymer matrix composites. Composites Science and Technology, **105**, 15–27 (2014).
DOI: 10.1016/j.compscitech.2014.08.032

[14] Xu S., Girouard N., Schueneman G., Shofner M. L., Meredith J. C.: Mechanical and thermal properties of waterborne epoxy composites containing cellulose nanocrystals. Polymer, **54**, 6589-6598 (2013).
DOI: 10.1016/j.polymer.2013.10.011

[15] Ruiz M. M., Cavaillé J. Y., Dufresne A., Graillat C., Gérard J-F.: New waterborne epoxy coatings based on cellulose nanofillers. Macromolecular Symposia, **169**, 211–222 (2001).
DOI: 10.1002/1521-3900(200105)169:1<211::AID-MASY211>3.0.CO;2-H

[16] Tang L., Weder C.: Cellulose whisker/epoxy resin nanocomposites. ACS Applied Materials and Interfaces, **2**, 1073–1080 (2010).
DOI: 10.1021/am900830h

[17] Lu J., Askeland P., Drzal L. T.: Surface modification of microfibrillated cellulose for epoxy composite applications. Polymer, **49**, 1285–1296 (2008).
DOI: 10.1016/j.polymer.2008.01.028

[18] Girouard N., Schueneman G. T., Shofner M. L., Meredith J. C.: Exploiting colloidal interfaces to increase dispersion, performance, and pot-life in cellulose nanocrystal/waterborne epoxy composites. Polymer, **68**, 111–121 (2015).
DOI: 10.1016/j.polymer.2015.05.009

[19] Gabr M. H., Elrahman M. A., Okubo K., Fujii T.: A study on mechanical properties of bacterial cellulose/epoxy reinforced by plain woven carbon fiber modified with liquid rubber. Composites Part A: Applied Science and Manufacturing, **41**, 1263–1271 (2010).
DOI: 10.1016/j.compositesa.2010.05.010

[20] Peng S. X., Moon R. J., Youngblood J. P.: Design and characterization of cellulose nanocrystal-enhanced epoxy hardeners. Green Materials, **2**, 193–205 (2014).
DOI: 10.1680/gmat.14.00015

[21] Ansari F., Galland S., Johansson M., Plummer C. J. G., Berglund L. A.: Cellulose nanofiber network for moisture stable, strong and ductile biocomposites and increased epoxy curing rate. Composites Part A: Applied Science and Manufacturing, **63**, 35–44 (2014).
DOI: 10.1016/j.compositesa.2014.03.017

[22] Barari B., Ellingham T. K., Ghamhia I. I., Pillai K. M., El-Hajjar R., Turng L-S., Sabo R.: Mechanical characterization of scalable cellulose nano-fiber based composites made using liquid composite molding process. Composites Part B: Engineering, **84**, 277–284 (2016).
DOI: 10.1016/j.compositesb.2015.08.040

[23] Miao C., Hamad W. Y.: Cellulose reinforced polymer composites and nanocomposites: A critical review. Cellulose, **20**, 2221–2262 (2013).
DOI: 10.1007/s10570-013-0007-3

[24] Karger-Kocsis J., Mahmood H., Pegoretti A.: Recent advances in fiber/matrix interphase engineering for polymer composites. Progress in Materials Science, **73**, 1–43 (2015).
DOI: 10.1016/j.pmatsci.2015.02.003

[25] Chen Y., Zhou X., Yin X., Lin Q., Zhu M.: A novel route to modify the interface of glass fiber-reinforced epoxy resin composite *via* bacterial cellulose. International Journal of Polymeric Materials and Polymeric Biomaterials, **63**, 221–227 (2013).
DOI: 10.1080/00914037.2013.830250

[26] Postek M. T., Moon R. J., Rudie A. W., Bilodeau M. A.: Production and applications of cellulose. Tappi Press. Peachtree Corners (2013).

[27] Rich M. J., Drzal L. T., Hunston D., Holmes G., McDonough W.: Round robin assessment of the single fiber fragmentation test. in 'Procedings of the American Society for Composites 17th Technical Conference, West Lafayette, USA' p.10 (2002)..

[28] Kelly A., Tyson W.: Tensile properties of fibre-reinforced metals: Copper/tungsten and copper/molybdenum. Journal of the Mechanics and Physics of Solids, **13**, 329–350 (1965).
DOI: 10.1016/0022-5096(65)90035-9

[29] Klein C. A.: Characteristic strength, Weibull modulus, and failure probability of fused silica glass. Optical Engineering, **48**, 113401/1–113401/11 (2009).
DOI: 10.1117/1.3265716

[30] Mullin J. V., Mazzio V. F.: The effects of matrix and interface modification on local fractures of carbon fibers in epoxy. Journal of the Mechanics and Physics of Solids, **20**, 391–394 (1972).
DOI: 10.1016/0022-5096(72)90016-6

[31] Zhou X-F., Nairn J. A., Wagner H. D.: Fiber–matrix adhesion from the single-fiber composite test: Nucleation of interfacial debonding. Composites Part A: Applied Science and Manufacturing, **30**, 1387–1400 (1999).
DOI: 10.1016/S1359-835X(99)00043-3

[32] Hashin Z.: Thermoelastic properties of fiber composites with imperfect interface. Mechanics of Materials, **8**, 333–348 (1990).
DOI: 10.1016/0167-6636(90)90051-G

[33] Nairn J. A.: Generalized shear-lag analysis including imperfect interfaces. Advanced Composites Letters, **13**, 263–274 (2004).

[34] Gao S-L., Mäder E.: Characterisation of interphase nanoscale property variations in glass fibre reinforced polypropylene and epoxy resin composites. Composites Part A: Applied Science and Manufacturing, **33**, 559–576 (2002).
DOI: 10.1016/S1359-835X(01)00134-8

[35] Madhukar M. S., Drzal L. T.: Fiber-matrix adhesion and its effect on composite mechanical properties: II. Longitudinal (0°) and transverse (90°) tensile and flexure behavior of graphite/epoxy composites. Journal of Composite Materials, **25**, 958–991 (1991).
DOI: 10.1177/002199839102500802

[36] Kinsella M., Murray D., Crane D., Mancinelli J., Kranjc M.: Mechanical properties of polymeric composites reinforced with high strength glass fibers. in '33rd International SAMPE Technical Conference, Seatle, USA' Vol. 33, 1644–1657 (2001).